Proposed Revisions to the Strength-Reduction Factor for Axially Loaded Members

Modifications correct anomalies for nonprestressed reinforced concrete members subjected to flexure and axial loads

by Rémy D. Lequesne and José A. Pincheira

Load factors and strength-reduction factors (ϕ-factors) are used to ensure acceptable reliability given expected failure modes; member importance; and unforeseeable variability in loads, material properties, construction, and engineering calculations.[1] In 1999, the basic ACI Building Code[2] load combination for only dead and live loads was $1.4D + 1.7L$ (refer to Notation section). In the current Code,[3] the basic load combinations are the maximum of $1.4D$ and $1.2D + 1.6L$. These were first adopted in 2002 and matched the load combinations in ASCE/SEI 7-02.[4] Per the commentary of ACI 318-02,[5] the "changes were made to further unify the design profession on one set of load factors and combinations, and to facilitate proportioning of concrete building structures that include members of materials other than concrete."

The 2002 ACI Building Code[5] also introduced new values for the ϕ-factors, with the objectives of:

- Associating the ϕ-factor to a measure of deformability;
- Simplifying and unifying the design of reinforced and prestressed concrete members subjected to axial forces and flexure[6]; and
- Ensuring members designed according to the 1999 and 2002 ACI Building Codes resulted in similar reliability.[7]

The ϕ-factors defined in the 1999 and 2011 ACI Building Codes for members subjected to flexure and axial force are shown in Table 1.

Table 1:
ϕ-factor definitions in 1999 and 2011 ACI Building Codes

ACI 318-99[2]	
$\phi_{99}P_n \le 0$	$\phi_{99} = 0.9$
$0 < \phi_{99}P_n < min\begin{bmatrix}\phi_{99}P_b \\ 0.1A_g f'_c\end{bmatrix}$	Linear variation with $\phi_{99}P_n$
$min\begin{bmatrix}\phi_{99}P_b \\ 0.1A_g f'_c\end{bmatrix} \le \phi_{99}P_n$	$\phi_{99} = 0.7$ (tied) (0.75 for spirally reinforced)
ACI 318-11[3]	
$\varepsilon_t \ge 0.005$	$\phi_{11} = 0.9$
$0.005 > \varepsilon_t > \varepsilon_{ty}$	Linear variation with ε_t
$\varepsilon_{ty} \ge \varepsilon_t$	$\phi_{11} = 0.65$ (tied) (0.75 for spirally reinforced)

Note: ε_{ty} is permitted to be taken as 0.002 for Grade 60 and prestressing steel

Concerns Regarding the Current ϕ-Factor Definition

Although design strengths calculated using the 1999 and 2011 ACI Building Codes are similar for most axially loaded members, the 2011 ACI Building Code provisions can result in much larger design strengths than permitted prior to 2002 for members with eccentricities larger than those at balanced strain conditions (that is, $\varepsilon_t > \varepsilon_{ty}$). For rectangular and circular sections, a larger design strength was justified on the basis that symmetrically reinforced members with yielding tensile reinforcement have greater deformation capacity than singly reinforced members.[6] However, the calculated strength can be substantially larger than permitted prior to 2002, especially for flanged sections. Moreover, the design interaction diagram calculated using the 2011 ACI Building Code provisions

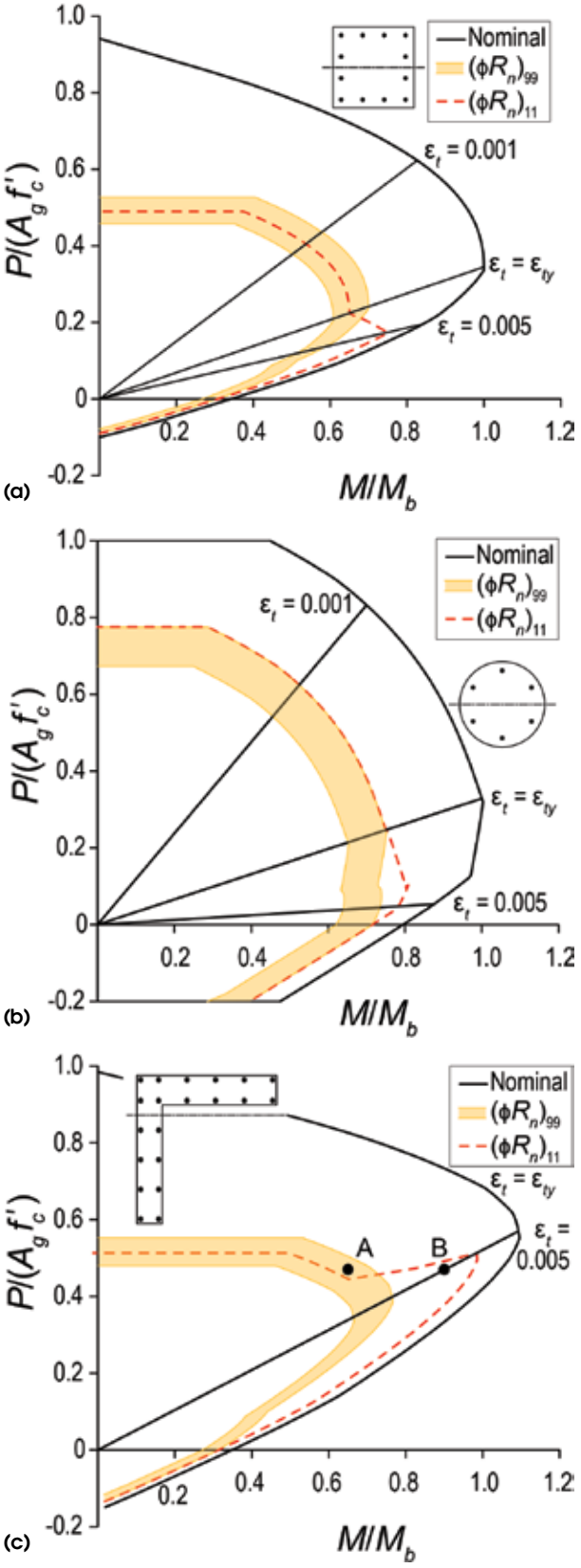

Fig. 1: Nominal and design interaction diagrams calculated with ϕ_{99} and ϕ_{11}: (a) square section with ρ_g = 1.0%; (b) circular section with ρ_g = 4.0%; and (c) L-shaped section with ρ_g = 1.06% and flange in compression

for sections with flanges in compression can unreasonably exhibit increased flexural and axial strength with increased eccentricity.

The aim of this article is to discuss the reasons for these anomalies and to propose specific changes to the current ϕ-factor definition for members subjected to flexure and axial loads. The issue raised in this article is separate from others previously identified (an odd interaction diagram shape for standard sections[8] and erroneous design strengths for certain prestressed sections[9]). This article does not discuss slenderness and shear effects.

Design Strength per the 1999 and 2011 ACI Building Codes

Rectangular and circular cross sections

Nominal and design interaction diagrams for a 24 in. (600 mm) square column with ρ_g = 1% and a 24 in. (600 mm) diameter circular cross section with ρ_g = 4% are shown in Fig. 1(a) and (b), respectively. Strengths were calculated using the 1999 and 2011 ACI Building Code provisions, f'_c = 6000 psi (40 MPa), Grade 60 (GR 400) reinforcement and Eq. (1)

$$(\phi R_n)_{99} = \phi_{99} R_n \, (LF_{11}/LF_{99}) \quad (1a)$$

$$(\phi R_n)_{11} = \phi_{11} R_n \quad (1b)$$

Because of the different load factors required by the 1999 and 2011 ACI Building Codes, the ϕ-factors cannot be compared vis-à-vis without modification. The ratio LF_{11}/LF_{99} in Eq. (1a) accounts for the different load factors and allows a direct comparison of the design strengths. Considering only dead and live loads, the ratio is calculated as the controlling load combination from 2011, either 1.4*D* or (1.2*D* + 1.6*L*), divided by (1.4*D* + 1.7*L*), the governing load combination from 1999. The LF_{11}/LF_{99} ratio is bounded by 0.87 and 1.0 as $L/(D + L)$ varies between 0 and 1.0. As a result, $(\phi R_n)_{99}$ is represented by a shaded region in Fig. 1 rather than one curve.

In Fig. 1, there is close agreement between $(\phi R_n)_{11}$ and $(\phi R_n)_{99}$ when $\varepsilon_t < \varepsilon_{ty} = 0.002$. However, $(\phi R_n)_{11}$ is generally greater than $(\phi R_n)_{99}$ for axial forces between 0 and P_b ($\varepsilon_t = \varepsilon_{ty}$) for both the square and circular cross sections. Although the increase in design strength was justified based on the high deformation capacity of tension-controlled members with symmetric longitudinal reinforcement,[6] the increase in calculated design strength can be substantial. For the square section with ρ_g = 1% and an eccentricity corresponding to ε_t = 0.005, $(\phi R_n)_{11}$ is 30 to 50% greater than $(\phi R_n)_{99}$, depending on the LF_{11}/LF_{99} ratio. For the circular section with ρ_g = 4%, $(\phi R_n)_{11}$ is up to 25% greater than $(\phi R_n)_{99}$. For these sections, the largest increase in calculated strength occurs at axial forces less than $0.2 A_g f'_c$.

Cross sections with flanges in compression

Consider the design interaction diagram shown in Fig. 1(c) for an L-shaped wall section found in practice calculated

when the flange is in compression. The wall has a depth of 39 in. (990 mm), a 43 in. (1090 mm) wide flange, $t_f = b_w = 7.9$ in. (200 mm), evenly distributed reinforcing bars, and $\rho_g = 1.06\%$. Material strengths of $f_c' = 4400$ psi (30.4 MPa) and $f_y = 61$ ksi (421 MPa) were used. The design interaction diagram, $(\phi R_n)_{11}$, shows that when $\varepsilon_{ty} \le \varepsilon_t \le 0.005$, increasing eccentricity results in increased axial and flexural strength. As a result, the design interaction diagram has a significantly different shape than the nominal interaction diagram, and $(\phi R_n)_{11}$ is up to 50% greater than $(\phi R_n)_{99}$ at nominal axial forces exceeding $0.4A_g f_c'$, where variability in concrete strength can have a large effect on sectional strength.

Furthermore, as shown in Fig. 1(c), the design strength can be ambiguous. Design of the wall for an axial force of $0.47A_g f_c'$ and a moment of $0.65M_b$ (Point A) would not be permitted, yet a larger moment of $0.9M_b$ would be permitted for the same axial force (Point B). In extreme cases, the design axial strength at $\varepsilon_t = 0.005$ can be calculated to exceed the maximum permitted axial force, $\phi_{11}P_{n,max}$. Design interaction diagrams calculated for slender C-, T-, and I-shaped walls tested in laboratories[10-12] exhibit the same characteristics as those in Fig. 1(c). Clearly, such a result was not intended when modifications were introduced to the ϕ-factor in 2002.

The increase in design strength as eccentricity increases is observed for wide flanged sections when the compression zone stress block extends into the web ($a > t_f$) and $\varepsilon_{ty} \le \varepsilon_t \le 0.005$. (This trend is independent of the shape of the stress block, as similar behavior occurs when a parabolic compressive stress distribution is assumed.) In such cases, $\phi_{11}P_n$ increases with eccentricity because ϕ_{11} increases at a proportionally higher rate than P_n decreases. The influence of flange thickness on this behavior is illustrated in Fig. 2(a). It is shown that for $t_f/h = 1/3$, $\phi_{11}P_n$ increases with eccentricity between Points A and B, when $a \ge t_f$, and decreases with eccentricity between Points B and C, when $a \le t_f$.

The influence of flange width on this behavior is illustrated in Fig. 2(b), where design interaction diagrams calculated using ϕ_{11} are plotted for four values of b_f/b_w. In each case shown, $a > t_f$ when $\varepsilon_{ty} \le \varepsilon_t \le 0.005$. For the wider flanged sections ($b_f/b_w = 4$ and 6 in Fig. 2(b)), $\phi_{11}P_n$ increases with eccentricity when $\varepsilon_{ty} \le \varepsilon_t \le 0.005$, whereas it does not for the sections with either no flange or a narrow flange ($b_f/b_w = 1$ and 2).

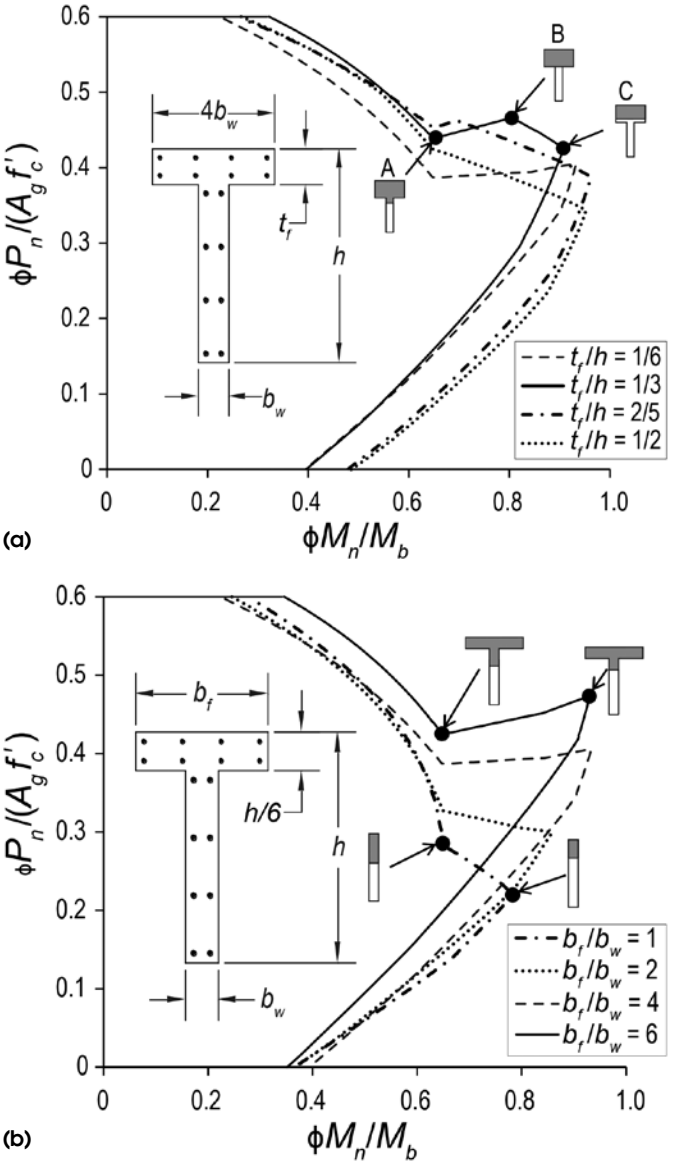

Fig. 2: Design interaction diagrams for T-shaped wall sections, calculated per 2011 ACI Building Code[3]: (a) for sections with flange thickness varying from 1/6 to 1/2 of the total section depth; and (b) for sections with flange width varying from 1 to 6 times the web thickness

Proposed Modification to the ϕ-Factor

To address the anomalies outlined above, changes to the 2011 ACI Building Code ϕ-factor definition are proposed. Specifically, the proposed changes were developed to:

- Provide reasonable calculated design strengths for nonprestressed members subjected to axial force and flexure;
- Produce a design interaction diagram with a shape consistent with the nominal response;
- Associate the ϕ-factor with a measure of deformability (such as ε_t); and
- Limit use of $\phi = 0.9$ to prudent design axial force levels.

The authors are not aware of tests of slender flanged walls (or flanged columns) subjected to axial forces greater than $0.1A_g f_c'$, and therefore see no evidence justifying use of $\phi = 0.9$ for flanged sections under larger axial loads, as currently permitted. Given the importance of axially loaded members within structural systems and the uncertainty associated with large axial forces, it seemed prudent to limit use of $\phi = 0.9$ to axial forces up to $0.1A_g f_c'$ until further test data are available.

To satisfy these requirements while also maintaining consistency with the current 2011 ACI Building Code provisions, the following ϕ-factor definition is proposed

$$\phi_{prop.(tied)} = 0.65 + 0.25\frac{\varepsilon_t - \varepsilon_{ty}}{\varepsilon_t^* - \varepsilon_{ty}} \le 0.9, \text{but not less than } 0.65 \quad (2a)$$

$$\phi_{prop.(spiral)} = 0.75 + 0.15\frac{\varepsilon_t - \varepsilon_{ty}}{\varepsilon_t^* - \varepsilon_{ty}} \le 0.9, \text{but not less than } 0.75 \quad (2b)$$

The proposed equations are identical to those in the current Code (and in the upcoming 2014 Code), except that the current tension control limit of 0.005 is replaced by ε_t^* in the denominator. The ε_t^* term is the greater of the net tensile strain calculated for $P_n = 0.1A_g f_c'$ and 0.005. Therefore, when $\varepsilon_t^* = 0.005$, $\phi_{prop.} = \phi_{11}$. Figure 3 shows the relationship between $\phi_{prop.}$ and ε_t for values of ε_t^* equal to 0.005, 0.008, and 0.012. As shown, the proposed equations result in a linear (as in the 2011 ACI Building Code) but more gradual increase in the ϕ-factor when the net tensile strain at $P_n = 0.1A_g f_c'$ is larger than 0.005. This proposal does not affect the design strength of members subjected to eccentricities less than those at balanced strain conditions or with $P_n \le 0.1A_g f_c'$.

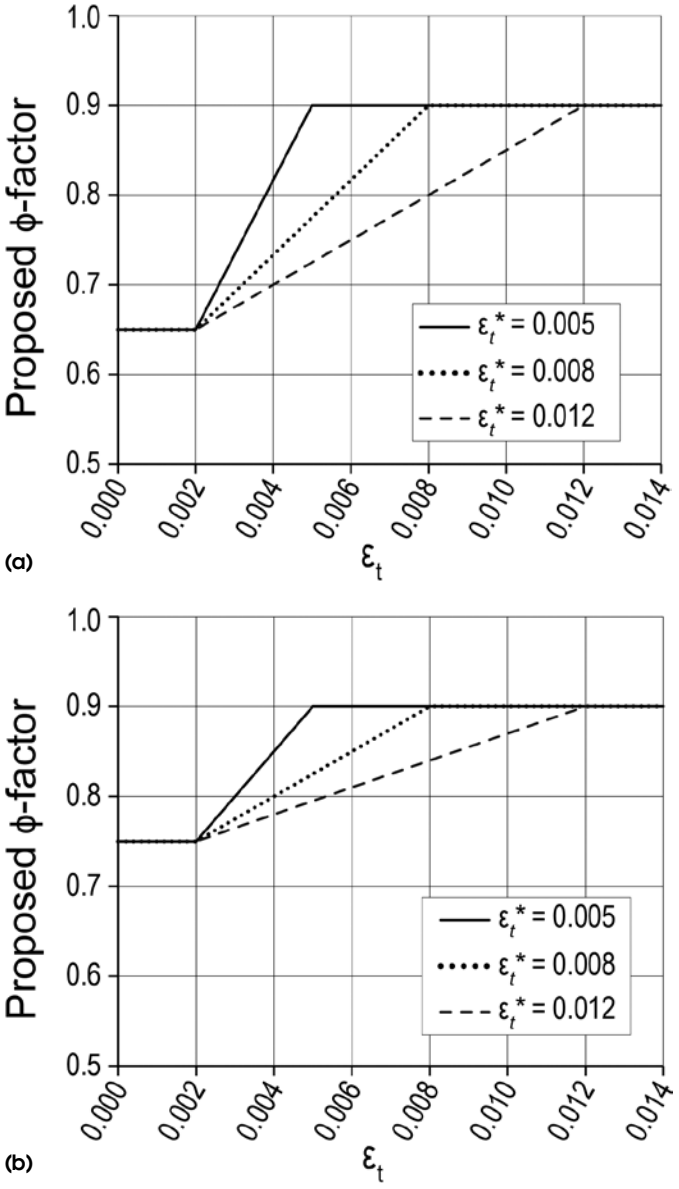

Fig. 3: Relationship between $\phi_{prop.}$ and ε_t for Grade 60 reinforcement and ε_t^* values of 0.005, 0.008, and 0.012: (a) for tied members; and (b) for spirally reinforced members

Note that use of $\phi_{prop.}$ requires no more effort than use of ϕ_{99}, and only one more calculation than use of ϕ_{11} (that is, calculation of ε_t^*). Calculation of $\phi_{prop.}$ can be done manually or using design software. Use of $P_n \le 0.1A_g f_c'$ in the proposed definition instead of $P_u \le 0.1A_g f_c'$, the axial load limit in the 2011 ACI Building Code for beams, simplifies calculation of the proposed ϕ-factor. Several options were considered when developing the proposed solution, including a reversion to the 1999 ACI Building Code provisions. However, they would have required a more significant departure from the current code format.

Comparison of Proposed Approach with ACI 318-99 and ACI 318-11

In Fig. 4, $(\phi R_n)_{prop.}$ is plotted with $(\phi R_n)_{99}$ and $(\phi R_n)_{11}$ for the same square, circular, and L-shaped sections as in Fig. 1. The variation of ϕ with P_n is also plotted. As shown, the proposed design interaction diagram, $(\phi R_n)_{prop.}$, retains the overall shape of the nominal diagram for all three cross sections. Most important, use of the proposed ϕ-factor for the flanged section (Fig. 4(c)) corrects the unreasonable features of the design diagram calculated with the current provisions. Also, the proposed design diagram leads to calculated design strengths comparable to $(\phi R_n)_{99}$ over the entire range of axial loads (particularly at axial loads greater than $0.3A_g f_c'$). Though not shown here, the design interaction diagrams for rectangular, circular, and flanged sections with a wide range of reinforcing ratios showed the same trends illustrated in Fig. 4.

To evaluate $\phi_{prop.}$, design strengths were calculated and compared to a database of results from 138 tests (the database and references are available at **http://www.engr.wisc.edu/cmsdocuments/cee-DBSLequesne_Pincheira.xlsx**). The database includes 105 rectangular columns, 28 circular columns, and five slender flanged wall specimens tested under monotonic or cyclic loading (biaxially loaded specimens were not included). For specimens with symmetric cross sections and reinforcement configurations tested under cyclic loading, the strength was taken as the average of the maximum resistance recorded in both loading directions. For T- and C-shaped sections, the strength was taken as the maximum resistance observed with the flange in compression. Properties of the specimens are summarized in Table 2. All specimens in the database have eccentricities greater than those corresponding to balanced strain conditions, and are thus within the range of interest for this study. As shown in Table 2, the rectangular columns were subjected to an average axial load of $0.21A_g f_c'$, higher than either the circular columns or

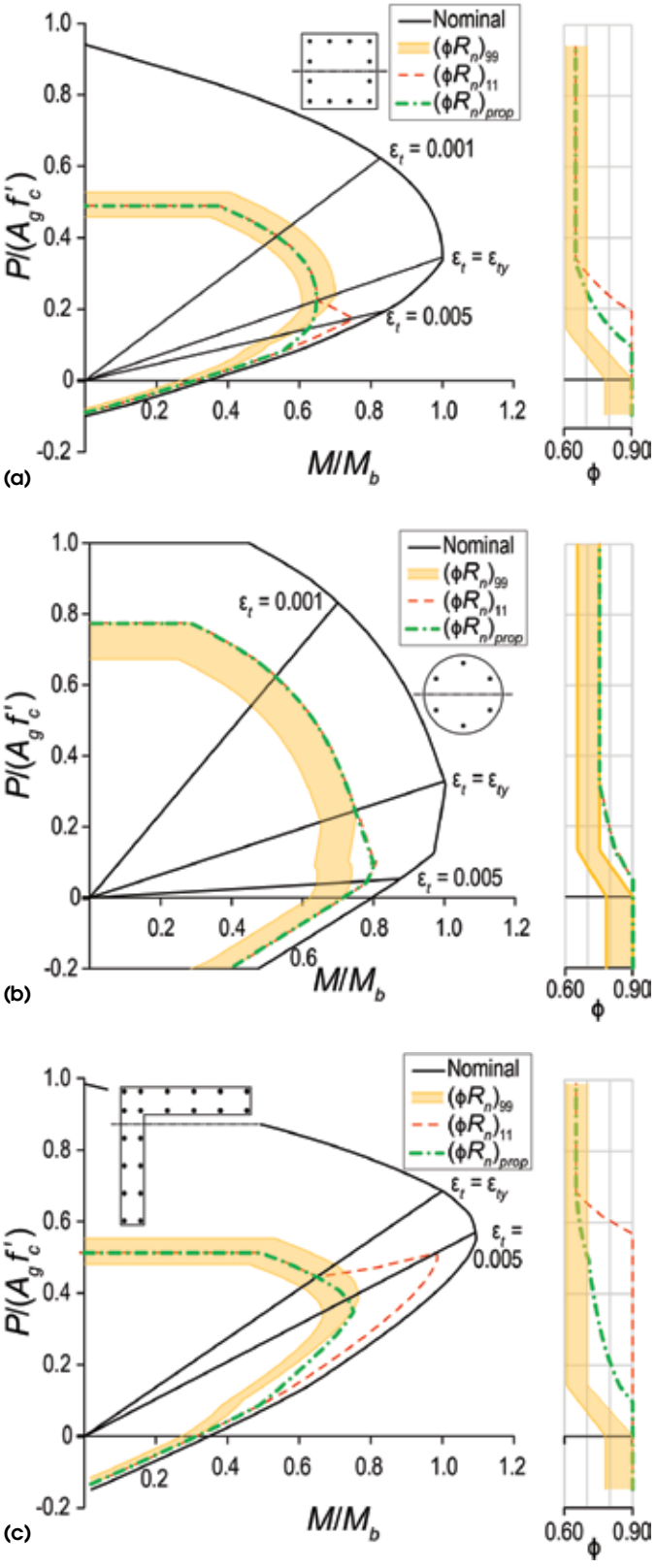

Fig. 4: Design interaction diagrams calculated using ϕ_{99}, ϕ_{11}, and $\phi_{prop.}$; variation of ϕ with P_n is shown to the right of each plot: (a) square section with ρ_g = 1.0%; (b) circular section with ρ_g = 4.0%; and (c) L-shaped section with ρ_g = 1.06% and flange in compression

Table 2:
Properties of specimens in database

Property	Mean	Range	
		Min.	Max.
Rectangular columns (105 specimens)			
h (in.)	11.6	2.5	24.0
b_w/h	1.02	0.63	1.76
ρ_g, %	2.3	1.2	4.8
f'_c, ksi	4.7	2.6	7.8
f_y, ksi	55.9	43.6	74.1
e/e_b	1.8	1.0	4.6
$P_{test}/(A_g f'_c)$, %	21	6.6	45
Circular columns (28 specimens)			
d (in.)	21.3	9.8	60.0
ρ_g, %	2.7	1.0	5.2
f'_c, ksi	4.9	3.4	7.6
f_y, ksi	64.6	44.7	69.2
e/e_b	2.5	1.1	4.8
$P_{test}/(A_g f'_c)$, %	17	6.8	56
Flanged walls (2 C-, 2 T-, and 1 I-shaped sections)			
h (in.)	48.6	36.0	75.0
b_f	50.4	36.0	60.0
b_f/b_w	10.6	9.0	12.0
t_f/h	0.08	0.05	0.08
ρ_g, %	1.2	0.8	1.8
f'_c, ksi	5.2	4.1	6.6
f_y, ksi	62.5	62.0	63.0
e/e_b	4.4	3.2	5.3
$P_{test}/(A_g f'_c)$, %	7.1	5.9	8.7

Note: 1 in. = 25 mm; 1 ksi = 6.9 MPa

flanged walls (which had average axial loads of $0.17A_g f'_c$ and $0.07A_g f'_c$, respectively). Note that the proposed ϕ-factor could not be evaluated against data from tests of slender flanged walls under axial loads near the balanced point because such data were not available.

For each specimen in the database, the nominal strength was calculated at the eccentricity reported at failure using measured material properties for f_y and f'_c. Elastic-plastic behavior was assumed for the steel reinforcement. Whitney's equivalent rectangular stress block was used to model the compression zone in the concrete, neglecting the effects of confinement. To compute ϕ_{11} and $\phi_{prop.}$, the yield strain corresponding to the nominal strength of the reinforcement was used.

Histograms of the ratios of the measured (experimental) and associated calculated strength values are shown in Fig. 5. Distributions for both the nominal strength ($\phi = 1$) and the design strength ($\phi = \phi_{prop.}$) are shown. For this database, the calculated mean, $\bar{x}$, of the measured nominal strength ratio is 1.12 and the standard deviation, σ_d, is 0.20. These are comparable to those of other datasets used in past reliability studies of normal strength, tension-controlled, tied columns ($\bar{x} = 1.05$ and $\sigma_d = 0.13$).[13] Using $\phi_{prop.}$, less than 5% of the specimens had measured-to-design strength ratios less than 1 (Fig. 5).

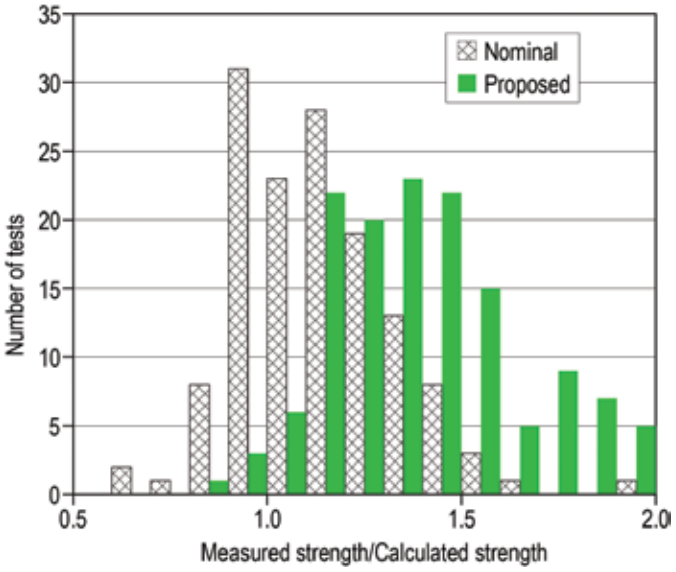

Fig. 5: Histograms of measured-calculated strength ratios for nominal strength and design strength using $\phi_{prop.}$

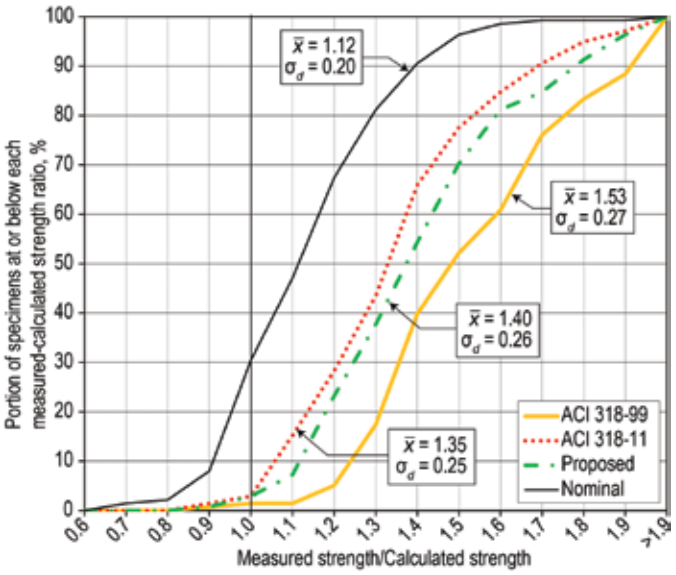

Fig. 6: Cumulative distributions of the measured-calculated strength ratios for specimens in database using ϕ_{99}, ϕ_{11}, $\phi_{prop.}$, and $\phi = 1.0$

Figure 6 shows a cumulative distribution of the measured-to-calculated strength ratios determined for nominal strength and design strengths calculated using ϕ_{99}, ϕ_{11}, and $\phi_{prop.}$. This comparison to laboratory data is not intended to evaluate whether $\phi_{prop.}$ appropriately accounts for construction tolerances and material variability, but rather to compare the conservatism of $\phi_{prop.}$ with that of ϕ_{11} and ϕ_{99}. For this dataset, the figure shows similar reliability for $\phi_{prop.}$ and ϕ_{11}, whereas use of ϕ_{99} results in greater conservatism. However, as shown previously, the proposed definition corrects the anomalies in the current (ACI 318-11) design interaction diagram for flanged sections with eccentricities near balanced strain conditions (Fig. 4(c)).

Summary and Conclusions

Modifications to the ϕ-factor definition for reinforced concrete members subjected to flexure and axial load are proposed. The current definition in ACI 318-11[3] and the proposed definition have the same format and provide similar reliability for rectangular and circular sections with common reinforcing ratios. For sections with flanges in compression, the proposed ϕ-factor corrects the anomalous design strengths calculated with the current provisions.

Acknowledgments

Supporting work done by Ann Thielmann and Brian Giese, former graduate students at the University of Wisconsin, Madison, is much appreciated. Thanks are also extended to Oguzhan Bayrak from the University of Texas at Austin, for sharing a database of high-strength concrete column test results that was used in the early stages of this study. The opinions and conclusions expressed in this article are those of the authors and do not necessarily represent those of the individuals mentioned herein.

References

1. MacGregor, J.G., "Load and Resistance Factors for Concrete Design," *ACI Journal Proceedings*, V. 80, No. 4, July-Aug. 1983, pp. 279-287.

2. ACI Committee 318, "Building Code Requirements for Structural Concrete (ACI 318-99) and Commentary," American Concrete Institute, Farmington Hills, MI, 1999, 392 pp.

3. ACI Committee 318, "Building Code Requirements for Structural Concrete (ACI 318-11) and Commentary," American Concrete Institute, Farmington Hills, MI, 2011, 503 pp.

4. ASCE/SEI 7-02, "Minimum Design Loads for Buildings and Other Structures," American Society of Civil Engineers, Reston, VA, 2002, 376 pp.

5. ACI Committee 318, "Building Code Requirements for Structural Concrete (ACI 318-02) and Commentary," American Concrete Institute, Farmington Hills, MI, 2002, 445 pp.

6. Mast, R.F., "Unified Design Provisions for Reinforced and Prestressed Concrete Flexural and Compression Members," *ACI Structural Journal*, V. 89, No. 2, Mar.-Apr. 1992, pp. 185-199.

7. Szerszen, M.M., and Nowak, A.S., "Calibration of Design Code for Buildings (ACI 318): Part 2—Reliability Analysis and

Resistance Factors," *ACI Structural Journal,* V. 100, No. 3, May-June 2003, pp. 383-391.

8. Gamble, W.L., "ϕ-Factors and Other Anomalies," *Concrete International,* V. 20, No. 8, Aug. 1998, pp. 56-58.

9. Naaman, A.E., "Limits of Reinforcement in 2002 ACI Code: Transition, Flaws, and Solution," *ACI Structural Journal*, V. 101, No. 2, Mar.-Apr. 2004, pp. 209-218.

10. Oesterle, R.G.; Aristizabal-Ochoa, J.D.; Fiorato, A.E.; Russell, H.G.; and Corley, W.G., *Earthquake Resistant Structural Walls - Test of Isolated Walls - Phase II*, Report No. ENV77-15333, National Science Foundation, Arlington, VA, 1979, 327 pp.

11. Sittipunt, C., and Wood, S.L., *Finite Element Analysis of Reinforced Concrete Shear Walls*, University of Illinois at Urbana-Champaign, Urbana, IL, 1993, 404 pp.

12. Thomsen IV, J.H., and Wallace, J.W., *Displacement-Based Design of RC Structural Walls: An Experimental Investigation of Walls with Rectangular and T-Shaped Cross-Sections,* Report CU/CEE-95/06, Clarkson University, Potsdam, NY, 1995, 353 pp.

13. MacGregor, J.G.; Mirza, S.A.; and Ellingwood, B., "Statistical Analysis of Resistance of Reinforced and Prestressed Concrete Members," *ACI Journal Proceedings*, V. 80, No. 3, May-June 1983, pp. 167-176.

Received and reviewed under Institute publication policies.

ACI member **Rémy D. Lequesne** is Assistant Professor of Civil, Environmental and Architectural Engineering at the University of Kansas, Lawrence, KS. He is Secretary of Joint ACI-ASCE Committee 408, Development and Splicing of Deformed Bars, and a member of Joint ACI-ASCE Committee 352, Joints and Connections in Monolithic Concrete Structures, and ACI Committee 544, Fiber-Reinforced Concrete. His research interests include the behavior and design of reinforced concrete members and earthquake-resistant design.

José A. Pincheira, FACI, is Associate Professor of Civil and Environmental Engineering at the University of Wisconsin-Madison. He is past Chair and member of ACI Committee 369, Seismic Repair and Rehabilitation. He is also a member of ACI Committee 374, Performance-Based Seismic Design of Concrete Buildings, and ACI Subcommittee 318-D, Flexure and Axial Loads (Structural Concrete Building Code). His research interests include the behavior and design of reinforced concrete members subjected to earthquakes and the seismic rehabilitation of concrete structures.

Notation

A_g = Gross cross-sectional area
a = Depth of compression stress block
b_f = Flange width
b_w = Web width
D = Dead load
d = Diameter
e = Eccentricity at failure
$e_b = M_b/P_b$
f_c' = Concrete compressive strength
f_y = Reinforcement yield stress
h = Height
L = Live load
LF_{11}/LF_{99} = Ratio of controlling load combinations in 2011 and 1999 ACI Building Codes for $L/(D + L)$ between 0 and 1.0
$M_b = M_n$ at balanced strain conditions
M_n = Nominal flexural strength
$P_b = P_n$ at balanced strain conditions
P_n = Nominal axial strength
P_{test} = Axial load at failure
R_n = Nominal strength
t_f = Flange thickness
$\bar{x}$ = Mean
ε_t = Net strain in extreme layer of longitudinal tension reinforcement
ε_t^* = ε_t calculated when $P_n = 0.1A_g f_c'$, but ≥ 0.005
ε_{ty} = Value of ε_t used to define a compression controlled section
ϕ = Strength-reduction factor
ϕ_{99} = ϕ-factor defined in 1999 ACI Building Code
ϕ_{11} = ϕ-factor defined in 2011 ACI Building Code
$\phi_{prop.}$ = Proposed ϕ-factor
ρ_g = Ratio of longitudinal steel reinforcement area to A_g
σ_d = Standard deviation